Myosin X is a downstream effector of PI(3)K during phagocytosis

Dianne Cox*, Jonathan S. Berg†, Michael Cammer‡, John O. Chinegwundoh*, Benjamin M. Dale*, Richard E. Cheney† and Steven Greenberg*§#

**Department of Medicine and §Pharmacology, Columbia University, 630 West 168th Street, New York, NY 10032, USA*
†Department of Cell and Molecular Physiology, UNC-Chapel Hill, Chapel Hill, NC 27599, USA
‡Department of Anatomy and Structural Biology, Albert Einstein College of Medicine Yeshiva University, Bronx, New York, NY 10461, USA
#e-mail: greenber@cuccfa.ccc.columbia.edu

Published online: 11 June 2002; DOI: 10.1038/ncb805

Phagocytosis is a phosphatidylinositol-3-OH-kinase (PI(3)K)-dependent process in macrophages. We identified Myo10 (Myosin-X), an unconventional myosin with pleckstrin homology (PH) domains, as a potential downstream target of PI(3)K. Myo10 was recruited to phagocytic cups in a wortmannin-sensitive manner. Expression of a truncation construct of Myo10 (Myo10 tail) in a macrophage cell line or cytosolic loading of anti-Myo10 antibodies in bovine alveolar macrophages inhibited phagocytosis. In contrast, expression of a Myo10 tail construct containing a point mutation in one of its PH domains failed to inhibit phagocytosis. Expression of Myo10 tail inhibited spreading, but not adhesion, on IgG-coated substrates, consistent with a function for Myo10 in pseudopod extension. We propose that Myo10 provides a molecular link between PI(3)K and pseudopod extension during phagocytosis.

Phagocytosis is the principal mechanism through which leukocytes engulf and kill pathogenic microbes. Phagocytosis through Fc receptors (FcγRs) requires actin assembly, pseudopod extension and phagosome closure (reviewed in refs 1,2). Recent data suggest that a lipid product of PI(3)K, phosphatidylinositol-3,4,5-trisphosphate (PIP_3), is required for the latter two events. First, after ligation of FcγRs in macrophages, there is a rapid and transient accumulation of PIP_3 *in vivo*[3,4] that is localized to phagocytic cups[5]. Second, inhibition of PI(3)K activity blocks pseudopod extension and phagocytosis without affecting actin polymerization[4]. Third, SHIP, an SH2 domain-containing inositol 5′-phosphatase that specifically hydrolyses PIP_3, is localized to phagocytic cups, where it has been implicated in terminating PIP_3 accumulation[5,6] and inhibiting phagocytosis[6]. Finally, expression of a catalytically inactive allele of SHIP in a macrophage cell line is associated with enhanced phagocytosis, similar to that seen in

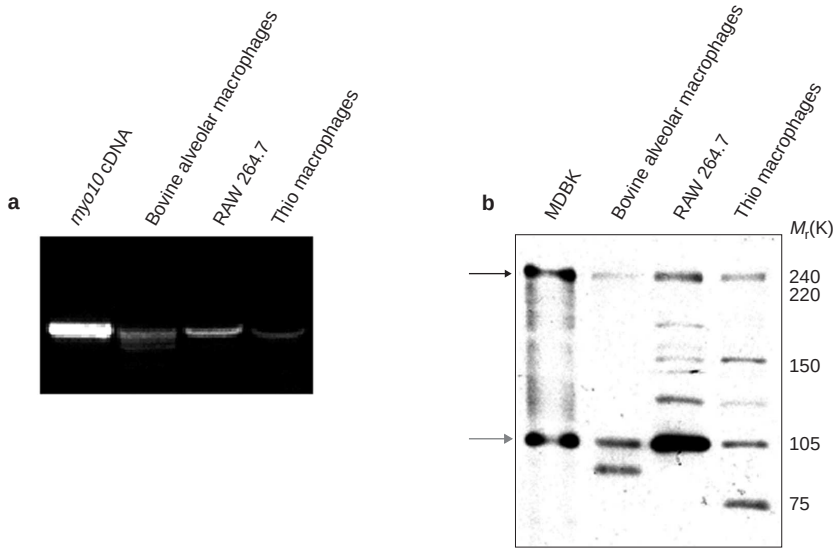

Figure 1 **Myo10 is present in macrophages. a**, RNA was isolated from equivalent cell numbers of the indicated cell types and RT-PCR was performed using Myo10-specific oligonucleotides that span intron–exon boundaries. Myo10 cDNA was used as a positive control. **b**, Whole cell lysates were prepared from equivalent cell numbers of the indicated cells. Detergent lysates were separated by SDS–PAGE and analysed by immunoblotting with an affinity-purified rabbit antibody against Myo10. Arrows indicate full-length Myo10 (black) or its major proteolytic fragment (grey).

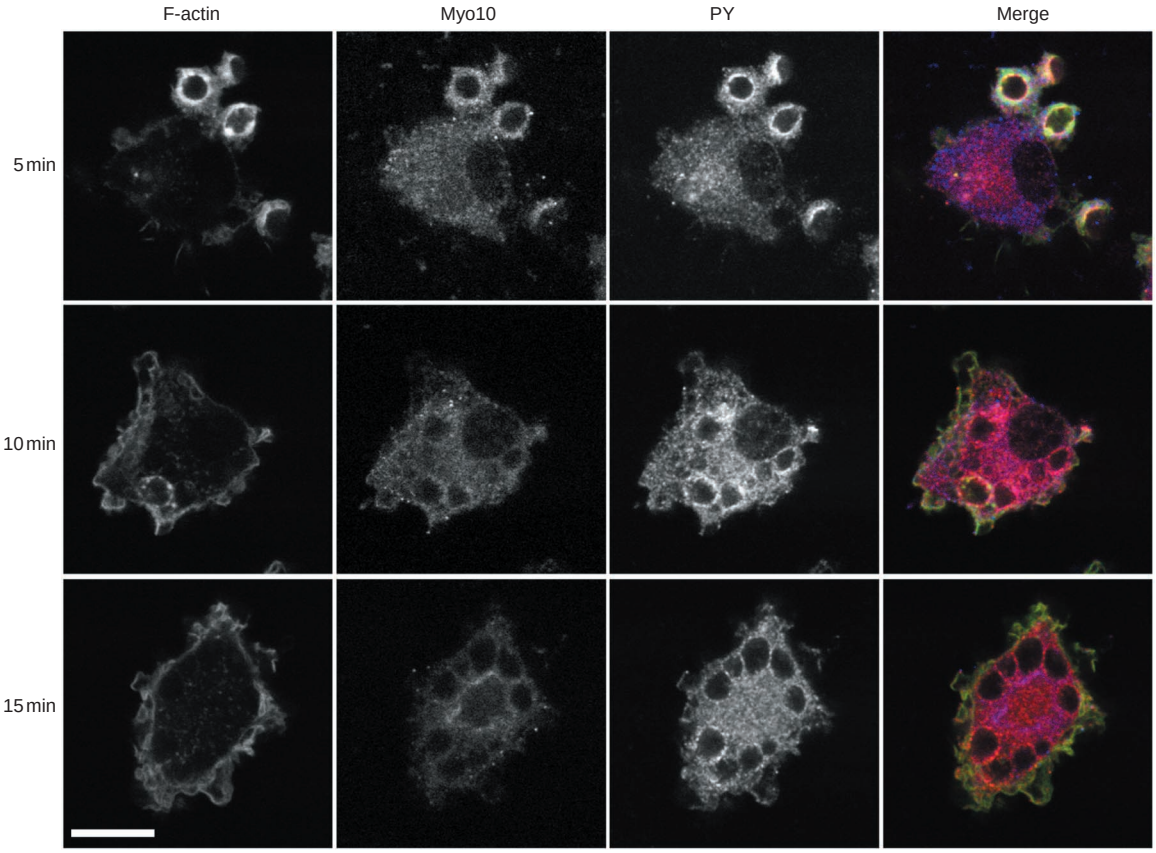

Figure 2 **Myo10 is localized to phagocytic cups.** Adherent bovine alveolar macrophages were incubated at 37 ° C with human IgG-coated erythrocytes for the indicated times. After fixation, cells were stained for F-actin, Myo10 and for phosphotyrosine (PY). In the merged image, Myo10 is blue, F-actin is green and PY is red. Scale bar, 10 μm.

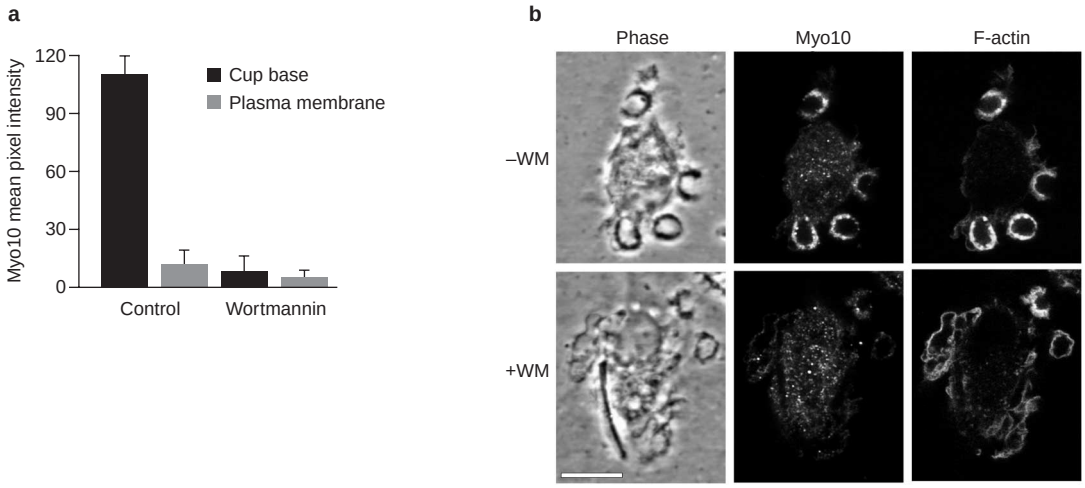

Figure 3 **Myo10 is recruited to phagocytic cups in a PI(3)K-dependent manner. a**, The enrichment of Myo10 in phagocytic cups in the presence or absence of 100 nM WM was quantified (see Methods). Data are expressed as the relative pixel intensity of Myo10 staining beneath attached particles, or Myo10 staining present in the cell periphery without bound particles. Data represent the mean ± SEM, $n = 30$. The differences between Myo10 staining in phagocytic cups in the presence and absence of WM were significant ($p < 0.005$). There was no significant difference between Myo10 staining in the periphery, either in the presence or absence of WM ($p > 0.05$). **b**, Adherent bovine alveolar macrophages were incubated in the absence (–WM) or presence (+WM) of 100 nM WM for 30 min before addition of human IgG-coated erythrocytes for 5 min at 37 °C. After fixation, cells were stained for F-actin and Myo10. Scale bar, 10 μm.

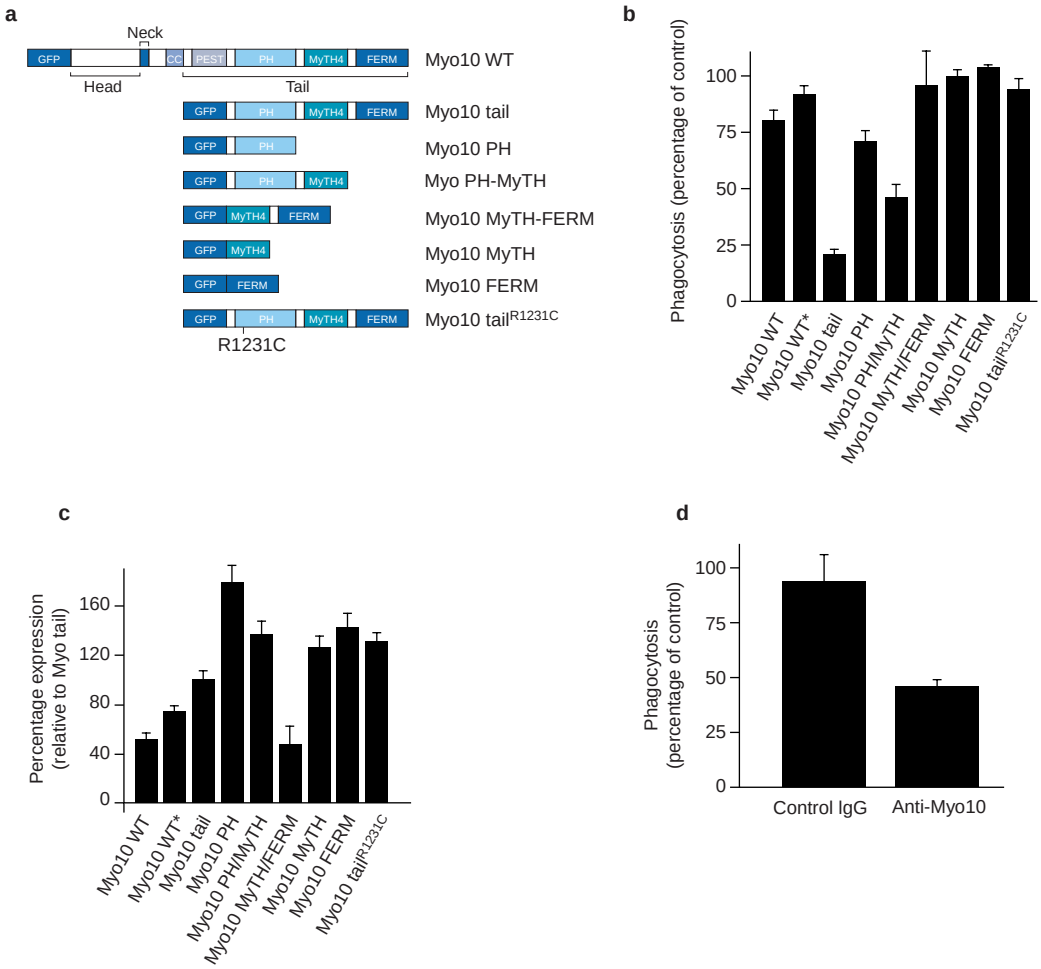

Figure 4 **Intact Myo10 function is required for FcγR-mediated phagocytosis.** **a**, A schematic representation of the various constructs used in this study. **b**, Adherent RAW LR5 cells transfected with the indicated constructs were treated with EIgG for 15 min at 37 °C. Phagocytosis was determined as the number of internalized EIgG per 100 transfectants and was expressed as a percentage of phagocytosis in non-expressing control cells on the same slide. The phagocytic index of non-expressing control cells was 317 ± 21. Data represent mean ± SEM, n = 3–4 independent experiments. **c**, Expression levels of the indicated constructs were determined by flow cytometry, except for expression of Myo10*, which was quantified by microspectrofluorometry (see Methods). The expression level of Myo10 tail was arbitrarily set to 100. **d**, Adherent bovine pulmonary alveolar macrophages were loaded with rhodamine–dextran and 0.4 mg ml^{-1} affinity purified anti-Myo10 or non-immune IgG, before incubation with EIgG. Phagocytosis, enumerated in rhodamine-positive IgG-loaded cells and unloaded controls, is expressed as ingested particles per IgG-loaded cells divided by unloaded cells × 100. The phagocytic index of unloaded controls was 987 ± 228. Data represent mean ± SEM, n = 3–4 independent experiments. Differences in phagocytosis between anti-Myo10 IgG- and control IgG-loaded cells were significant ($p < 0.005$).

SHIP$^{-/-}$ macrophages[6]. The reciprocal roles of PI(3)K and SHIP in phagocytosis indicates that PIP_3 is a critical effector in the signalling pathway that induces phagocytosis and pseudopod extension. Because PIP_3 and other phosphoinositides bind to PH-domain containing proteins, we sought to identify PH domain-containing protein targets of PIP_3 that are recruited locally during phagocytosis.

A genetic screen for PH domains with potential high affinity for PIP_3 identified multiple candidates, including the unconventional myosin, Myo10 (ref. 7). Myo10 is expressed in essentially all vertebrates, from frogs to humans, but does not seem to be present in invertebrates. The tail of Myo10 has three tandem PH domains, the second of which binds PIP_3 (ref. 7). Interestingly, a requirement for unconventional myosins in phagocytosis had been proposed previously[8,9]. Various myosin isoforms are associated with phagocytic cups in both *Dictyostelium discoideum* and mouse macrophages[8,9]. Addition of butanedione monoxime, a general myosin ATPase inhibitor, blocks phagocytosis at a stage similar to that seen with PI(3)K inhibitors[9]. Deletion of several different myosin isoforms in *Dictyostelium* results in a reduced efficiency of phagocytosis[10]. Deletion of myosin VII, in particular, results in selective defects in phagocytosis and dynamic adhesion[11,12]. Family tree analysis demonstrated that *Dictyostelium* myosin VII is structurally similar to vertebrate myosins VIIa, VIIb, X and XV. All these proteins contain MyTH4 domains of uncertain function and carboxy-terminal FERM domains[13]; however, of these, only Myo10 is widely expressed[14–16]. Myo10 is enriched in actin-rich protrusions, including lamellipodia and filopodia, in several cells types[16,17]. Although mRNA for Myo10 is detected in peripheral blood leukocytes[16], its expression and function in macrophages has not been reported. In this study we examined the function of Myo10 in FcγR-mediated phagocytosis.

Results

Myo10 is expressed in macrophages. We determined whether Myo10 is expressed in macrophages. *myo10* mRNA was present in

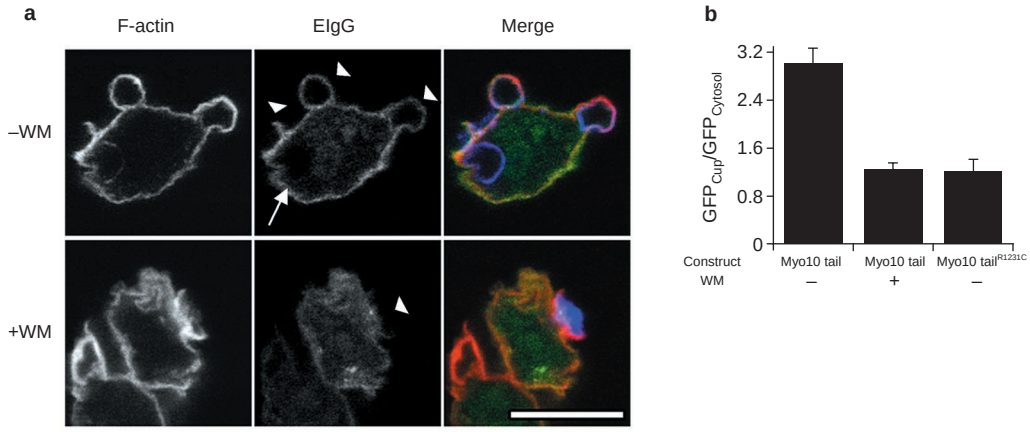

Figure 5 **Myo10 tail is present in phagocytic cups. a**, RAW LR5 cells transfected with Myo10 tail were incubated in the absence (–WM) or presence (+WM) of 100 nM WM for 30 min before addition of EIgG for 5 min at 37 °C. After fixation, cells were stained for F-actin and EIgG. In the merged image, Myo10 tail is green, F-actin is red, and EIgG is blue. Scale bar, 10 μm. Myo10 tail is present in newly-formed phagocytic cups in the absence of WM (top, arrowheads) but is absent in fully internalized phagosomes (top, arrows) or in phagosomes formed in the presence of WM (bottom, arrowheads). **b**, Quantification of Myo10 tail or Myo10 tail^{R1231C} in phagocytic cups in the presence or absence of 100 nM WM. Data are expressed as a ratio of relative pixel intensity of GFP fluorescence beneath attached particles to the relative pixel intensity of GFP in the cytosol of the same cell. Data represent the mean ± SEM, n = 10–22 cells from two independent experiments.

macrophages from multiple sources, as determined by reverse transcription (RT)-PCR using Myo10-specific oligonucleotides (Fig.1a). To confirm that Myo10 protein was present, immunoblots of macrophage lysates were probed with an affinity-purified polyclonal antibody raised against the head domain of Myo10 (Fig. 1b). Myo10 was detected as a band with a relative molecular mass (M_r) of 250,000 (250K), corresponding to full-length Myo10; a major proteolytic fragment of 110K was consistently detected, despite the use of multiple protease inhibitors (Fig. 1b). For comparison, bands of similar molecular weights were detected in lysates derived from Madin Darby Bovine Kidney cells[16]. The other bands present in lanes derived from macrophage lysates are most likely breakdown products of intact Myo10, consistent with the avid proteolytic activity of macrophages. Myo10 was also expressed in human monocyte-derived macrophages (data not shown). These data indicate that Myo10 is expressed in macrophages derived from multiple vertebrate species.

Myo10 is recruited to phagocytic cups in a PI(3)K-dependent manner. A previous study showed that Myo10 was enriched in cell surface protrusions[16]. Because cell surface protrusions in the form of pseudopods are generated during phagocytosis, we determined the distribution of Myo10 in bovine pulmonary alveolar macrophages (PAMs) undergoing phagocytosis. Myo10 was enriched in early phagosomes, coinciding with the appearance F-actin-rich pseudopods (Fig. 2). Loss of phagosomal Myo10 immunoreactivity occurred with kinetics similar to those of phagosomal F-actin, whereas phosphotyrosine immunoreactivity was apparent even in late phagosomes (Fig. 2), indicating that derecruitment of Myo10 from phagosomes was selective. Quantitative immunofluorescence microscopy identified an eightfold enrichment of Myo10 in phagocytic cups (Fig. 3). Incubation of PAMs with wortmannin (WM), a potent inhibitor of PI(3)Ks, blocked the enrichment of Myo10 in phagocytic cups (Fig. 3). These data indicate that the recruitment of Myo10 during phagocytosis is dependent on PI(3)K activity.

Myo10 is required for optimal FcγR-mediated phagocytosis. Because Myo10 was present in phagocytic cups, and a requirement for myosin ATPase activity in phagocytosis has been reported[9], we examined the function of Myo10 in phagocytosis. Expression of a green fluorescent protein (GFP)-tagged truncation fragment of Myo10 containing the tail of Myo10 (Myo10 tail) in a sub-line of RAW 264.7 cells resulted in a 79% ± 2% reduction of EIgG (antibody-coated erythrocytes) phagocytosis, compared to non-expressing control cells ($p < 0.001$). We determined which domains of Myo10 were responsible for the inhibition of phagocytosis by expressing GFP-tagged versions of the different domains of Myo10 (Fig. 4a). Expression of only those constructs that contained the PH domains of Myo10 inhibited phagocytosis (Fig. 4b). In contrast, expression of GFP-tagged full-length Myo10 (Myo10 WT), or untagged full-length Myo10 (Myo10 WT*), did not result in a significant inhibition of phagocytosis (Fig. 4b). The lack of an effect on phagocytosis by some of the constructs was not caused by lower expression levels, as these constructs were expressed at higher levels than Myo10 tail (Fig. 4c). The inhibition of phagocytosis by Myo10 tail was unlikely to be a result of simple sequestration of PIP_3, because expression of Myo10 tail inhibited phagocytosis to a greater degree than did expression of the isolated tandem Myo10 PH domains, which were expressed at even higher levels (Fig. 4b,c). The effect of expression of Myo10 tail on phagocytosis was specific, as it did not inhibit membrane ruffling in response to 12-*O*-tetradecanoylphorbol-13-acetate (TPA; data not shown).

Because the second PH domain of Myo10 binds to PIP_3 (ref. 7), we tested its role in phagocytosis by substituting Cys for Arg 1231 in Myo10 tail. This Arg corresponds to a conserved residue in the β_2 strand of PH domain-containing proteins, such as Gap1 and Btk, that is required for selective, high-affinity binding to lipid products of PI(3)K[18,19]. Cells expressing Myo10 tail^{R1231C} ingested EIgG 94% ± 5% as efficiently as non-expressing controls (Fig. 4b), indicating that Arg 1231 is required for the inhibition of phagocytosis by Myo10 tail.

To confirm that Myo10 is required for phagocytosis, we introduced affinity-purified antibodies raised against amino acids 1–952 of Myo10 into the cytosol of bovine alveolar macrophages. The presence of these antibodies, but not control antibody, inhibited phagocytosis (Fig. 4d). Thus, Myo10 function is required for optimal phagocytosis in primary lung macrophages.

The localization of Myo10 tail was examined by immunofluorescence microscopy to determine whether Myo10 tail was recruited to phagocytic cups. Myo10 tail was present at the plasma membrane and phagosomal membranes of transfected cells (Fig. 5a), as were

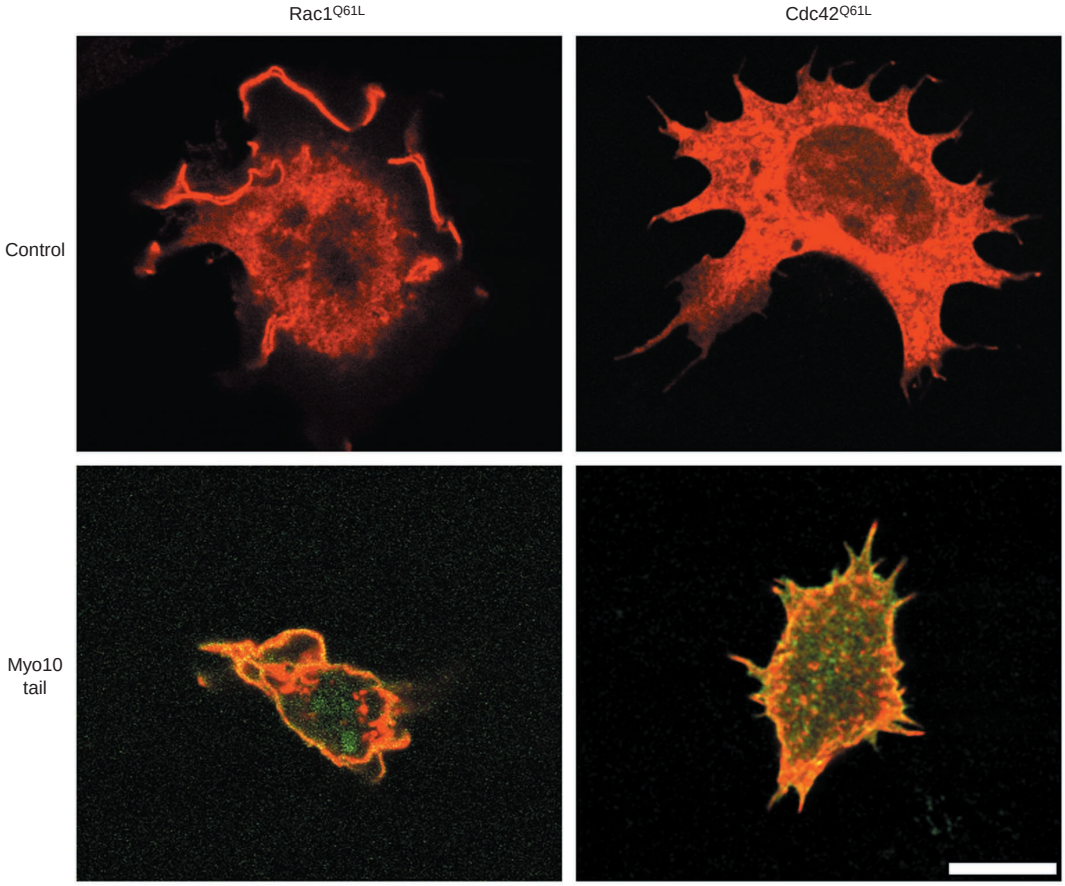

Figure 6 **Expression of Myo10 tail does not inhibit Rac1- or Cdc42-mediated actin assembly.** RAW LR5 cells were transfected with plasmids encoding Myc–Rac1^{Q61L} or Myc–Cdc42^{Q61L} alone, or with Myo10 tail, and then fixed and stained for Myc. Scale bar, 10 μm.

all of the constructs containing the PH domains of Myo10 (data not shown). Constructs lacking the PH domain were not targeted to the plasma membrane or phagosomal membranes (data not shown). In common with endogenous Myo10, Myo10 tail was less concentrated in the phagosomal membrane in the presence of WM (Fig. 5b). The persistence of some degree of Myo10 tail staining in the phagosome, despite the presence of WM, may be caused by its relatively high level of expression. This may also explain the constitutive association of Myo10 tail with areas of plasma membrane that were not actively engaged in phagocytosis. Further enrichment of Myo10 tail in the phagosome may not be possible because of a limiting number of Myo10 binding sites at the phagosomal membrane.

Although Myo10 tail was present beneath bound EIgG, it did not inhibit the formation of F-actin-rich phagocytic cups (Fig. 5a). The effect of expression of Myo10 tail on other actin-dependent events was also determined. Expression of Myo10 tail did not inhibit membrane ruffles stimulated by expression of Rac1^{Q61L} or filopodia stimulated by expression of Cdc42^{Q61L} (Fig. 6). The phenotype observed by expression of Myo10 tail (that is, inhibition of phagocytosis without an effect on actin assembly) was similar to the phenotype seen after inhibition of PI(3)K[4,20].

Myo10 is required for maximal pseudopod extension during phagocytosis. Inhibition of PI(3)K activity in macrophages inhibits the ingestion of large, but not small, particles that have been coated with antibody, as a result of the requirement for greater pseudopod extension in the ingestion of large beads[4]. To examine the function of Myo10 in pseudopod extension, we tested whether inhibition of Myo10 activity had an effect on the phagocytosis of antibody-coated beads of varying sizes. There was no difference in the phagocytosis of 2-μm antibody-coated beads between control and Myo10 tail-expressing cells; however, there was a reduction in the phagocytosis of 6-μm antibody-coated beads in Myo10-expressing cells (Fig. 7a). Similarly, bovine alveolar macrophages loaded with antibodies against Myo10 showed a reduction in the phagocytosis of 6-μm, but not 2-μm, antibody-coated beads (Fig. 7b). These results are consistent with a function for Myo10 in pseudopod extension.

Because pseudopod extension *per se* is difficult to quantify, we measured the rate and extent of spreading of Myo10 tail-expressing cells on antibody-coated substrates. Expression of Myo10 tail inhibited the spreading of cells on antibody-coated substrates when compared to non-expressing cells (Fig. 8a). Although deletion of another unconventional myosin, Myo7, results in decreased phagocytosis as a result of decreased particle adhesion in *Dictyostelium*[12], this was not the case for Myo10 inhibition in macrophages. There was no difference in the ability of Myo10 tail-expressing cells to bind to EIgG when compared to non-expressing control cells (8.5 ± 1.1 versus 8.1 ± 0.9 particles per cell, respectively). In addition, flow cytometry identified no difference in the surface expression of FcγRs in cells expressing Myo10 tail when compared to non-expressing control cells (data not shown). As an index of the strength of adhesion to the antibody, we used interference reflection microscopy (IRM). In IRM images, areas of the cell that are separated from the substrate by less than 50 nm appear darker than the background, whereas areas of the cell that are more than 100 nm above the substrate appear lighter than the background[21]. There was no apparent difference in the IRM patterns of Myo10

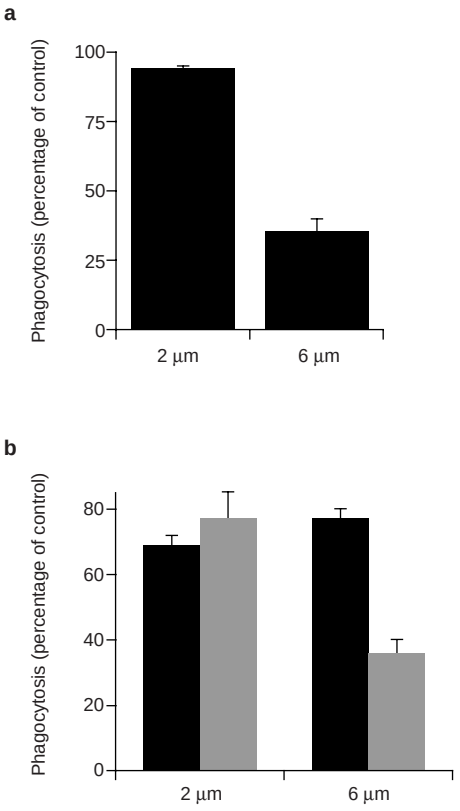

Figure 7 **Inhibition of phagocytosis by Myo10 tail expression is dependent on particle size. a**, RAW LR5 cells transfected with Myo10 tail were incubated with either 2- or 6-μm IgG-coated beads for 30 min at 37 °C. Phagocytosis was determined as the number of internalized beads per 100 transfectants and expressed as a percentage of phagocytosis in non-expressing control cells on the same slide. Data represent mean ± SEM, n = 3–5 independent experiments. Differences in the phagocytosis of 6-μm beads by Myo10 tail-expressing cells and non-expressing controls were significant ($p < 0.005$). **b**, Adherent bovine alveolar macrophages were permeabilized in the presence of 0.4 mg ml^{-1} affinity purified anti-Myo10 IgG (grey bars) or non-immune IgG (black bars) and rhodamine–dextran (as a marker of permeabilization) before incubation with either 2- or 6-μm IgG-coated beads for 30 min at 37 °C. Phagocytosis is expressed as ingested particles per IgG-loaded cells divided by unloaded control cells × 100. Data represent mean ± SEM, n = 3 independent experiments. The differences in phagocytosis of 6-μm beads between anti-Myo10 IgG-loaded and control IgG-loaded cells were significant ($p < 0.005$).

tail-expressing cells when compared to non-expressing cells (Fig. 8b,c), indicating that in Myo10 tail-expressing cells, the closeness of apposition of FcγRs to the antibody ligand was unaltered. Collectively, these data are consistent with a function for Myo10 in spreading on, but not adhesion to, antibodies.

Discussion

The inhibition of phagocytosis at similar stages by the PI(3)K inhibitor, WM, and the myosin ATPase inhibitor, BDM, suggests a functional convergence between PI(3)K-generated signals and myosins. Our study shows that Myo10 is recruited to phagocytic cups in a PI(3)K-dependent manner and that inhibition of Myo10 activity results in impaired phagocytosis and spreading on antibody-coated surfaces. Thus, we have implicated Myo10 as a molecular link between PI(3)K activation and pseudopod extension during phagocytosis.

At least 18 different classes of unconventional myosins have been identified[13,22]. Multiple myosins are found in phagocytic cups; in vertebrates, these include myosins IC, II, V, IXB[8,9] and X (this study). Of the former, only myosins I and II have been implicated in phagocytosis. A role for members of the myosin I family in phagocytosis has been suggested by studies in *Dictyostelium*. However, deletion of several class I myosins in *Dictyostelium* resulted in only minor defects in phagocytosis. Targeted deletion of either myoB or myoC results in reductions in phagocytosis[23], pinocytosis[23] and membrane recycling (myoB; ref. 24), whereas disruption of myoK, a small myosin whose motor domain resembles that of myosin I, results in decreased phagocytosis, chemotaxis, and cortical tension[25].

Class I myosins are phosphorylated by the PAK family of serine/threonine kinases, which results in the activation of actin-dependent ATPase activity[26,27]. Members of the PAK family are direct targets of Cdc42 and Rac, suggesting that myosin I motor activity and actin assembly may be coordinately regulated. However, vertebrate myosins I lack the consensus site for PAK phosphorylation, suggesting other means of regulation exist. Studies have implicated (conventional) myosin II in phagocytosis by human neutrophils[28], but not by macrophages[29].

Additional myosins may be expected to contribute to phagocytosis in vertebrates. For example, Class I, V, VI and VII myosins have been shown to be involved in vesicle transport (reviewed in ref. 30) and local exocytosis of endocytic vesicles is required for pseudopod extension during phagocytosis[4,31]. Myosin VII has been shown to be required for phagocytosis and dynamic cell adhesion in *Dictyostelium*[11] and myosin VIIa is involved in opsin transport in vertebrate photoreceptors[32]. However, myosin VIIa is not expressed in mouse macrophages[9] and myosin VIIb has a highly restricted distribution[15]. Recently, myosin Vb has been shown to interact with Rab11 and to be required for exocytosis from the transferrin receptor-containing recycling compartment in fibroblasts[33]. The vesicles that are required for phagocytosis and pseudopod extension in macrophages share these characteristics[31,34] and recycling from this compartment in other cells requires PI(3)K activity[35,36]. It is not known whether myosin Vb contributes to phagocytosis.

Myo10 is structurally related to myosins VIIa, VIIb and VX, and all contain MyTH and FERM domains. In contrast to myosins VIIa, VIIb and XV, which have a relatively restricted tissue distribution, the distribution of Myo10 is widespread[14–16]. However, Myo10 is unique in that it is the only vertebrate myosin to contain PH domains. The presence of a PH domain in Myo10 that binds with high affinity to PIP_3 (ref. 7) makes it a potential direct molecular target of PI(3)K; the data provided herein support this hypothesis. First, Myo10 is recruited to phagocytic cups in a WM-inhibitable fashion. Second, only those Myo10 constructs that contained PH domains conferred plasma membrane targeting and phagocytic inhibition. Finally, mutation of Arg 1341, the residue predicted to confer high-affinity PIP_3 binding[7], abrogated inhibition by Myo10 tail. However, we cannot eliminate the possibility that other PI(3)K-generated signals during phagocytosis contribute indirectly to either the localization or function of Myo10.

Little is known about the requirement for PI(3)K in phagocytosis by lower organisms. Phagocytosis has been extensively characterized in *Dictyostelium*, but the role of PI(3)K in phagocytosis in this organism is unclear. In one study, deletion of two of the three genes in *Dictyostelium* with homology to the p110 catalytic subunit of mammalian PI(3)K resulted in no reduction in phagocytosis[37]. In another study, deletion of the same two genes resulted in a 50% decrease in phagocytosis[38]. In a third study, incubation of *Dictyostelium* with WM had no effect on the phagocytosis of 1-μm latex beads[39]. It should be noted that the size of the particles used in the *Dictyostelium* studies were small, and even in macrophages, the phagocytosis of small particles shows little sensitivity to WM[4]. There are no reports concerning the requirement for PI(3)K in phagocytosis by organisms such as *Drosophila melanogaster* or

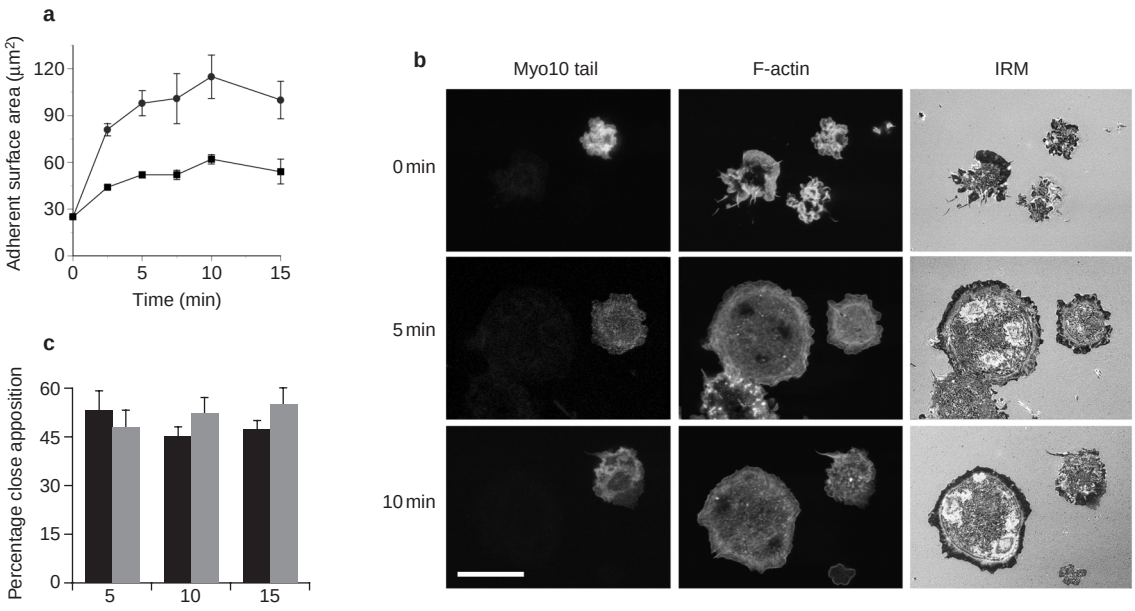

Figure 8 **Expression of Myo10 tail inhibits spreading, but not adhesion, of macrophages on IgG-coated substrates.** RAW LR5 cells transfected with Myo10 tail were incubated at 4 °C on IgG-coated coverslips to allow adhesion to occur, before further incubation at 37 °C for the indicated times. After fixation, cells were stained for the presence of F-actin. **a**, Data are expressed as mean adherent surface areas for GFP-expressing cells (squares) or non-expressing cells (circles). Data represent mean ± SEM, $n = 3$ independent experiments. **b**, Representative images of GFP (Myo10 tail), F-actin and interference reflection microscopy (IRM) of cells spreading for the indicated times are shown. Scale bar, 10 μm. **c**, The strength of adhesion was estimated by determining the percentage of close apposition (see Methods). Each bar represents the mean ratios derived from 10 individual Myo10 tail-expressing (grey bars) or non-expressing (black bars) cells.

Caenorhabditis elegans. Phagocytosis of yeast or red blood cells by ascidian haemocytes, immune cells of the sea squirt, is a PI(3)K-dependent process[40]. It is not known whether PI(3)K is required for pseudopod extension during phagocytosis in these cells. Class X myosins have not been identified in the complete genomes of *Saccharomyces cerevisiae*, *C. elegans* or *Drosophila*, suggesting that Myo10 is expressed only in vertebrates[16]. It may be possible that pseudopod extension during phagocytosis in lower organisms is mediated by one or more different unconventional myosins that lack PH domains. Recruitment of these unconventional myosins may or may not be PI(3)K-dependent.

Although the PH domain of Myo10 seems to be required for recruitment of Myo10 to the plasma membrane and for phagocytosis, the FERM domain also seems to contribute to its phagocytic function. This was demonstrated by the reduced ability of the Myo10 PH and Myo10 PH-MyTH constructs, which lack the FERM domain, to inhibit phagocytosis (Fig. 4b). FERM domains in other proteins have been shown to interact with multiple ligands, including several transmembrane glycoproteins and phosphatidylinositol-4,5-bisphosphate[41]. It is possible that the FERM domain of Myo10 may stabilize membrane–cytoskeletal interactions that occur during pseudopod extension, perhaps by binding to these ligands[42]. Our data do not indicate a function for the FERM domain in plasma membrane targeting, as the presence of this domain in Myo10 tail constructs did not enhance either plasma membrane or phagosomal membrane targeting. It is possible that the Myo10 FERM domain participates in intra- or inter-molecular associations with other domains in Myo10, or mediates multiple uncharacterized protein–protein interactions required for phagocytosis.

We do not yet know the precise function of Myo10 in pseudopod extension and phagocytosis. Unlike *Dictyostelium* myosin VII, Myo10 does not directly participate in FcγR-directed dynamic adhesion (see Fig. 8b). Given the apparent requirement for the head of Myo10 in phagocytosis (this study) and its association with filopodia[43], it is likely that some interaction with F-actin is important for its function. In common with all myosins, other than myosin VI, Myo10 is a motor protein that moves towards the barbed ends of actin filaments[44]. The velocity of recombinant Myo10 head on actin filaments is approximately 0.5 μm sec^{-1}, which is comparable to that of myosin V and II (ref. 44). The biochemical profile of Myo10 suggests that it a non-processive motor[44]. Thus, in contrast to myosin V, it is less likely to function as a vesicle transporter. Indeed, Myo10 does not seem to be involved in the delivery of FcγRs to the cell surface (this study), nor does it affect the delivery of endocytic vesicles to the forming phagosome (see Supplementary Information, Fig. S1) or influence the extent of macropinocytosis (see Supplementary Information, Fig. S2). We speculate that Myo10 molecules bind to PIP_3 generated at the plasma membrane through their PH domains, which functions to recruit Myo10 to sites of phagocytosis. Myo10 would then engage locally generated actin filaments and contribute to bulk plasma membrane movement in the direction of the barbed ends (that is, towards pseudopodial tips). Because intraphagosomal PIP_3 has restricted mobility[5], Myo10 may serve as a PIP_3-dependent force transducer, functioning to couple movement of the actin-based cytoskeleton with outward movement of the plasma membrane. This interpretation predicts that the base of the phagosome is anchored, relative to the nascent pseudopods. □

Methods

Cell and reagents

RAW LR5 cells were derived from RAW 264.7 cells[45]. Bovine alveolar macrophages were isolated from cow lungs (obtained after non-survival surgery) by segmental broncho-alveolar lavage. Thioglycollate-elicited peritoneal macrophages were isolated by peritoneal lavage from mice 4 days after intraperitoneal injection of thioglycollate broth[46]. Cells were maintained in RPMI medium containing 10% foetal calf serum, 100 μg ml^{-1} streptomycin and 100U ml^{-1} penicillin G (Sigma, St Louis, MO). Human mononuclear cells were isolated by density gradient centrifugation of blood obtained from the New York Blood Center (New York, NY). Macrophages were isolated by adherence and maintained for 6 days of culture in human AB blood-type serum[47]. The affinity-purified rabbit anti-bovine Myo10 antibody used in this study was characterized previously[16]. PY99, a phosphotyrosine-specific monoclonal antibody, was from Santa Cruz Biotechnology (Santa Cruz, CA). The rabbit anti-sheep erythrocyte

antibody was from Cappel (Aurora, OH). The horseradish peroxidase-conjugated donkey antibody against rabbit IgG and $F(Ab')_2$ fragments, Cy5-conjugated donkey anti-rabbit and anti-human IgG were from Jackson ImmunoResearch Laboratories (West Grove, PA). Rhodamine–phalloidin, Alexa 488–phalloidin, Alexa 568-conjugated goat anti-rabbit and anti-mouse antibodies were from Molecular Probes (Eugene, OR). Glass beads (425–600 μm) were from Sigma. The superfect transfection reagent was from Qiagen (Valencia, CA). RNAzol B was from Tel-Test, Inc. (Friendswood, TX).

Construction of plasmids and transfection of cells

Myo10 (nucleotides 1–6588) was subcloned into pcDNA3.1 from Invitrogen (Carlsbad, CA). GFP-tagged constructs were created by subcloning PCR-generated inserts coding for nucleotides: 1–6588 (amino acids 1–2052) of Myo10 wild-type, 3700–6588 (amino acids 1159–2052) of Myo10 tail, 3700–4783 (amino acids 1159–1520) of Myo10 PH, 3700–5398 (amino acids 1159–1797) of Myo10 PH-MyTH, 4783–5612 (amino acids 1521–2052) of Myo10 MyTH-FERM, 4783–5451 (amino acids 1521–1743) of Myo10 MyTH and 5452–6588 (amino acids 1744–2052) of Myo10 FERM into pEGFP from Clontech (San Diego, CA). Mutation of Arg 1231 to Cys in Myo10 tail, to form Myo10 $tail^{R1231C}$, was generated using the QuikChange site-directed mutagenesis kit from Stratagene (La Jolla, CA). All constructs were verified by DNA sequencing. Transfection of plasmids into RAW LR5 cells was performed using Superfect, in accordance with the manufacturer's instructions. Expression levels of transfected GFP-tagged constructs were determined using flow cytometry.

myo10 expression

For RT-PCR, RNA was isolated from 5×10^6 bovine alveolar, human monocyte derived, thioglycollate-elicited peritoneal macrophages and RAW LR5 macrophages using RNAzol B, according to manufacturer's guidelines. RT-PCR was performed using Titan one-tube RT-PCR kit from Pharmingen BD (San Diego, CA). The primers used were designed against sequences of Myo10 that were conserved in mice, cows and humans, that lacked homology to other myosins and that spanned an intron–exon boundary: 5′-GTTTGAACAGGCCCACGAAG-3′ and 5′-CCTGGAGCTGCCCTGGCTGC-3′. For immunoblotting, detergent lysates were prepared from 5×10^6 bovine alveolar, human monocyte-derived, thioglycollate-elicited peritoneal macrophages and RAW LR5 macrophages, separated by SDS–polyacrylamide gel electrophoresis (PAGE), and electrophoretically transferred[48]. Blots were probed with an affinity-purified rabbit antibody raised against the head domain of Myo10 and a horseradish peroxidase-conjugated donkey anti-rabbit antibody before visualization by enhanced chemiluminescence.

Phagocytosis and spreading assays

1×10^6 sheep erythrocytes opsonized with rabbit IgG (EIgG) were added to RAW LR5 cells that had been previously transfected with the indicated constructs and incubated at either 4 °C (for binding) or 37 °C for 15 min (for phagocytosis), as described previously[45]. After fixation and permeabilization, cells were stained with an Alexa 568-conjugated anti-rabbit antibody to detect particles. Thirty GFP-positive cells per coverslip were scored for association or phagocytosis. Thirty non-expressing cells on the same coverslip functioned as controls. Cells from a minimum of five separate microscopic fields per coverslip were analysed. For introduction of the anti-Myo10 antibody into macrophage cytosol, adherent bovine alveolar macrophages were transiently permeabilized with glass beads in the presence of rhodamine–dextran and either 0.4 mg ml^{-1} affinity purified rabbit anti-bovine Myo10 or a control rabbit antibody[49]. After a 1-h recovery, 1×10^6 EIgG was added and incubated at 37°C for 15 min. Phagocytosis was determined for 30 rhodamine-positive EIgG-loaded cells and compared to 30 rhodamine-negative cells on the same coverslip. Spreading of macrophages on human IgG was performed essentially as described[4]. RAW LR5 cells were transfected with the indicated constructs and allowed to adhere to 13-mm^2 round coverslips coated with 1 mg ml^{-1} human IgG at 4 °C. Cells were allowed to spread for varying times at 37 °C before fixation and staining for F-actin, using rhodamine–phalloidin to facilitate delineation of cell margins. The average of 2 cell diameters in close contact with the coverslips was determined and the apparent adherent cell surface area was calculated. The adherent surface areas of 30 expressing and non-expressing controls per coverslip were measured.

Fluorescence microscopy and image analysis

Human IgG-coated erythrocytes were prepared by biotinylating sheep erythrocytes before incubation in 10 μg ml^{-1} streptavidin and subsequent incubation in 10 μg ml^{-1} biotinylated human IgG. Adherent bovine alveolar macrophages were incubated with human IgG-coated erythrocytes at 4 °C to allow particle binding, then incubation at 37 °C for various times before fixation in 3.7% formaldehyde. Cells were permeabilized in 0.2% Triton-X100 and stained for F-actin with Alexa 488–phalloidin. Myo10 was detected with an affinity-purified rabbit anti-Myo10 antibody before incubation with a Cy5-conjugated anti-rabbit antibody. The presence of phosphotyrosine residues was detected with the monoclonal antibody PY 99 and an Alexa 568-conjugated anti-mouse antibody. To quantify endogenous Myo10 localization during phagocytosis, adherent bovine alveolar macrophages were incubated with human IgG-coated erythrocytes in the presence or absence of 100 nM WM. Cells were stained for F-actin with Alexa 488–phalloidin, for Myo10 with anti-Myo10 and an Alexa 568-conjugated anti-rabbit antibody, and for the particles with a Cy5-conjugated anti-human antibody. Images were collected on a BioRad Radiance 2000 confocal microscope. Images were imported into Scion Image (Scion Corporation, Frederick, MD). A 2-μm line was drawn at the base of a phagocytic cup (identified by the presence of F-actin beneath a bound particle) and the mean pixel intensities of Myo10 staining in the presence or absence of WM was determined for 30 cells. In the same cells, mean pixel intensities were also determined for regions of the plasma membrane that lacked an associated particle. To determine the relative distributions of Myo10 tail constructs in phagosomes and the cytosol of transfected cells, the relative pixel intensity of GFP fluorescence beneath attached particles was determined, as described above, and compared to the GFP fluorescence in the cytosol of the same cell.

Interference reflection microscopy

IRM of cells spreading on IgG-coated coverslips was performed with a BioRad Radiance 2000 confocal microscope equipped with polarizing filters to remove a central reflection and to allow for imaging across the entire field. The method of using a confocal microscope for IRM has been described previously[50]. We developed an estimate of the strength of ligand adhesion using images obtained by IRM and calculating the percentage of pixels corresponding to regions of close apposition. Images were selected for analysis if they contained a GFP-positive cell and an adjacent GFP-negative cell. Using Image-J (http://rsb.info.nih.gov/ij/), the boundaries of individual cells were traced manually and a greyscale histogram was derived for each cell, which was then imported into Microsoft Excel. All thresholds for histograms were set at a greyscale value of 46. Values below this corresponded to regions that appeared black by IRM. A ratio was derived for each cell (percentage close apposition) that consisted of the sum of pixels, 46 or less, divided by the total number of pixels contained within the boundaries of the cell.

RECEIVED 27 SEPTEMBER 2001; REVISED 2 APRIL 2002; ACCEPTED 19 APRIL 2002;
PUBLISHED 11 JUNE 2002.

1. Greenberg, S. Modular components of phagocytosis. *J. Leuk. Biol.* **66,** 712–717 (1999).
2. Greenberg, S. *Fc receptor-mediated phagocytosis* in *Phagocytosis: The Host*, Vol. 5 (ed. Gordon, S.) 149–191 (JAI, Stamford, 1999).
3. Ninomiya, N. *et al.* Involvement of phosphatidylinositol 3-kinase in Fc_γ receptor signaling. *J. Biol. Chem.* **269,** 22732–22737 (1994).
4. Cox, D., Tseng, C.-C., Bjekic, G. & Greenberg, S. A requirement for phosphatidylinositol 3-kinase in pseudopod extension. *J. Biol. Chem.* **274,** 1240–1247 (1999).
5. Marshall, J. G. *et al.* Restricted accumulation of phosphatidylinositol 3-kinase products in a plasmalemmal subdomain during Fc_γ receptor-mediated phagocytosis. *J. Cell Biol.* **153,** 1369–1380 (2001).
6. Cox, D., Dale, B. M., Kashiwada, M., Helgason, C. D. & Greenberg, S. A regulatory role for Src homology 2 domain-containing inositol 5′- phosphatase (SHIP) in phagocytosis mediated by Fc γ receptors and complement receptor 3 ($\alpha_M\beta_2$; CD11b/CD18). *J. Exp. Med.* **193,** 61–71 (2001).
7. Isakoff, S. J. *et al.* Identification and analysis of PH domain-containing targets of phosphatidylinositol 3-kinase using a novel *in vivo* assay in yeast. *EMBO J.* **17,** 5374–5387 (1998).
8. Allen, L. A. H. & Aderem, A. A role for MARCKS, the α isozyme of protein kinase C and myosin I in zymosan phagocytosis by macrophages. *J. Exp. Med.* **182,** 829–840 (1995).
9. Swanson, J. A. *et al.* A contractile activity that closes phagosomes in macrophages. *J. Cell Sci.* **112,** 307–316 (1999).
10. Jung, G., Wu, X. & Hammer, J. A. 3rd. *Dictyostelium* mutants lacking multiple classic myosin I isoforms reveal combinations of shared and distinct functions. *J. Cell Biol.* **133,** 305–323 (1996).
11. Titus, M. A. A class VII unconventional myosin is required for phagocytosis. *Curr. Biol.* **9,** 1297–1303 (1999).
12. Tuxworth, R. I. *et al.* A role for myosin VII in dynamic cell adhesion. *Curr. Biol.* **11,** 318–329 (2001).
13. Hodge, T. & Cope, M. J. A myosin family tree. *J. Cell Sci.* **113,** 3353–3354 (2000).
14. Hasson, T. *et al.* Effects of *shaker-1* mutations on myosin-VIIa protein and mRNA expression. *Cell Motil. Cytoskeleton* **37,** 127–138 (1997).
15. Chen, Z. Y. *et al.* Myosin-VIIb, a novel unconventional myosin, is a constituent of microvilli in transporting epithelia. *Genomics* **72,** 285–296 (2001).
16. Berg, J. S., Derfler, B. H., Pennisi, C. M., Corey, D. P. & Cheney, R. E. Myosin-X, a novel myosin with pleckstrin homology domains, associates with regions of dynamic actin. *J. Cell Sci.* **113,** 3439–3451 (2000).
17. Berg, J. S. & Cheney, R. E. Myosin-X is an unconventional myosin that undergoes intrafilopodial motility. *Nature Cell Biol.* **4,** 246–250 (2002).
18. Salim, K. *et al.* Distinct specificity in the recognition of phosphoinositides by the pleckstrin homology domains of dynamin and Bruton's tyrosine kinase. *EMBO J.* **15,** 6241–6250 (1996).
19. Fukuda, M. & Mikoshiba, K. Structure–function relationships of the mouse $Gap1^m$. Determination of the inositol 1,3,4,5-tetrakisphophate-binding domain. *J. Biol. Chem.* **271,** 18838–18842 (1996).
20. Araki, N., Johnson, M. T. & Swanson, J. A. A role for phosphoinositide 3-kinase in the completion of macropinocytosis and phagocytosis by macrophages. *J. Cell Biol.* **135,** 1249–1260 (1996).
21. Izzard, C. S. & Lochner, L. R. Cell-to-substrate contacts in living fibroblasts: an interference reflexion study with an evaluation of the technique. *J. Cell Sci.* **21,** 129–159 (1976).
22. Berg, J. S., Powell, B. C. & Cheney, R. E. A millennial myosin census. *Mol. Biol. Cell* **12,** 780–794 (2001).
23. Jung, G., Wu, X. & Hammer, J. A. 3rd. *Dictyostelium* mutants lacking multiple classic myosin I isoforms reveal combinations of shared and distinct functions. *J. Cell Biol.* **133,** 305–323 (1996).
24. Neuhaus, E. M. & Soldati, T. A myosin I is involved in membrane recycling from early endosomes. *J. Cell Biol.* **150,** 1013–1026 (2000).
25. Schwarz, E. C., Neuhaus, E. M., Kistler, C., Henkel, A. W. & Soldati, T. *Dictyostelium* myosin IK is involved in the maintenance of cortical tension and affects motility and phagocytosis. *J. Cell Sci.* **113,** 621–633 (2000).
26. Wu, C. *et al.* Activation of myosin-I by members of the Ste20p protein kinase family. *J. Biol. Chem.* **271,** 31787–31790 (1996).
27. Szczepanowska, J. *et al.* Identification by mass spectrometry of the phosphorylated residue responsible for activation of the catalytic domain of myosin I heavy chain kinase, a member of the PAK/STE20 family. *Proc. Natl Acad. Sci. USA* **94,** 8503–8508 (1997).
28. Mansfield, P. J., Shayman, J. A. & Boxer, L. A. Regulation of polymorphonuclear leukocyte phagocytosis by myosin light chain kinase after activation of mitogen-activated protein kinase. *Blood* **95,** 2407–2412 (2000).
29. de Lanerolle, P., Gorgas, G., X., L. & Schluns, K. Myosin light chain phosphorylation does not increase during yeast phagocytosis by macrophages. *J. Biol. Chem.* **268,** 16883–16886 (1993).
30. Tuxworth, R. I. & Titus, M. A. Unconventional myosins: anchors in the membrane traffic relay. *Traffic* **1,** 11–18 (2000).
31. Bajno, L. *et al.* Focal exocytosis of VAMP3-containing vesicles at sites of phagosome formation. *J. Cell Biol.* **149,** 697–706 (2000).
32. Liu, X., Udovichenko, I. P., Brown, S. D., Steel, K. P. & Williams, D. S. Myosin VIIa participates in opsin transport through the photoreceptor cilium. *J. Neurosci.* **19,** 6267–6274 (1999).
33. Lapierre, L. A. *et al.* Myosin Vb is associated with plasma membrane recycling systems. *Mol. Biol. Cell* **12,** 1843–1857 (2001).
34. Cox, D., Lee, D. J., Dale, B. M., Calafat, J. & Greenberg, S. A Rab11-containing rapidly recycling compartment in macrophages that promotes phagocytosis. *Proc. Natl Acad. Sci. USA* **97,** 680–685 (2000).

35. Shepherd, P. R., Soos, M. A. & Siddle, K. Inhibitors of phosphoinositide 3-kinase block exocytosis but not endocytosis of transferrin receptors in 3T3-L1 adipocytes. *Biochim. Biophys. Acta* **211,** 535–539 (1995).
36. Spiro, D. J., Boll, W., Kirchhausen, T. & Wessling-Resnick, M. Wortmannin alters the transferrin receptor endocytic pathway *in vivo* and *in vitro*. *Mol. Biol. Cell* **7,** 355–367 (1996).
37. Buczynski, G. *et al.* Inactivation of two *Dictyostelium discoideum* genes, *DdPIK1* and *DdPIK2*, encoding proteins related to mammalian phosphatidylinositide 3-kinases, results in defects in endocytosis, lysosome to postlysosome transport, and actin cytoskeleton organization. *J. Cell Biol.* **136,** 1271–1286 (1997).
38. Zhou, K., Pandol, S., Bokoch, G. & Traynor-Kaplan, A. E. Disruption of *Dictyostelium* PI3K genes reduces [^{32}P]phosphatidylinositol 3,4 bisphosphate and [^{32}P]phosphatidylinositol trisphosphate levels, alters F-actin distribution and impairs pinocytosis. *J. Cell Sci.* **111,** 283–294 (1998).
39. Seastone, D. J., Lee, E., Bush, J., Knecht, D. & Cardelli, J. Overexpression of a novel rho family GTPase, RacC, induces unusual actin-based structures and positively affects phagocytosis in *Dictyostelium discoideum*. *Mol. Biol. Cell* **9,** 2891–2904 (1998).
40. Ishikawa, G., Azumi, K. & Yokosawa, H. Involvement of tyrosine kinase and phosphatidylinositol 3-kinase in phagocytosis by ascidian hemocytes. *Comp. Biochem. Physiol. A Mol. Integr. Physiol.* **125,** 351–357 (2000).
41. Chishti, A. H. *et al.* The FERM domain: a unique module involved in the linkage of cytoplasmic proteins to the membrane. *Trends Biochem. Sci.* **23,** 281–282 (1998).
42. Hamada, K., Shimizu, T., Matsui, T., Tsukita, S. & Hakoshima, T. Structural basis of the membrane-targeting and unmasking mechanisms of the radixin FERM domain. *EMBO J.* **19,** 4449–4462 (2000).
43. Berg, S. & Cheney, R. E. Myosin-X is an unconventional myosin that undergoes intrafilopodial motility. *Nature Cell Biol.* **4,** 246–250 (2002).
44. Homma, K., Saito, J., Ikebe, R. & Ikebe, M. Motor Function and Regulation of Myosin X. *J. Biol. Chem.* **276,** 34348–34354 (2001).
45. Cox, D. *et al.* Requirements for both Rac1 and Cdc42 in membrane ruffling and phagocytosis in leukocytes. *J. Exp. Med.* **186,** 1487–1494 (1997).
46. Di Virgilio, F., Meyer, B. C., Greenberg, S. & Silverstein, S. C. Fc receptor-mediated phagocytosis occurs in macrophages at exceedingly low cytosolic Ca^{2+} levels. *J. Cell Biol.* **106,** 657–666 (1988).
47. El Khoury, J. *et al.* Macrophages adhere to glucose-modified basement membrane collagen IV via their scavenger receptors. *J. Biol. Chem.* **269,** 10197–10200 (1994).
48. Greenberg, S., Chang, P. & Silverstein, S. C. Tyrosine phosphorylation of the γ subunit of Fc_γ receptors, $p72^{syk}$, and paxillin during Fc receptor-mediated phagocytosis in macrophages. *J. Biol. Chem.* **269,** 3897–3902 (1994).
49. McNeil, P. L. & Warder, E. Glass beads load macromolecules into living cells. *J. Cell Sci.* **88,** 669–678 (1987).
50. Smith, C. L. Cytoskeletal movements and substrate interactions during initiation of neurite outgrowth by sympathetic neurons *in vitro*. *J. Neurosci.* **14,** 384–398 (1994).

ACKNOWLEDGMENTS

This work was supported by National Institutes of Health grants HL54164 to S.G., K01 AR02158 to D.C. and DC03299 to R.E.C.

Correspondence and requests for material should be addressed to S.G.

Supplementary Information is available on *Nature Cell Biology*'s website (http://cellbio.nature.com).

COMPETING FINANCIAL INTERESTS

The authors declare that they have no competing financial interests.

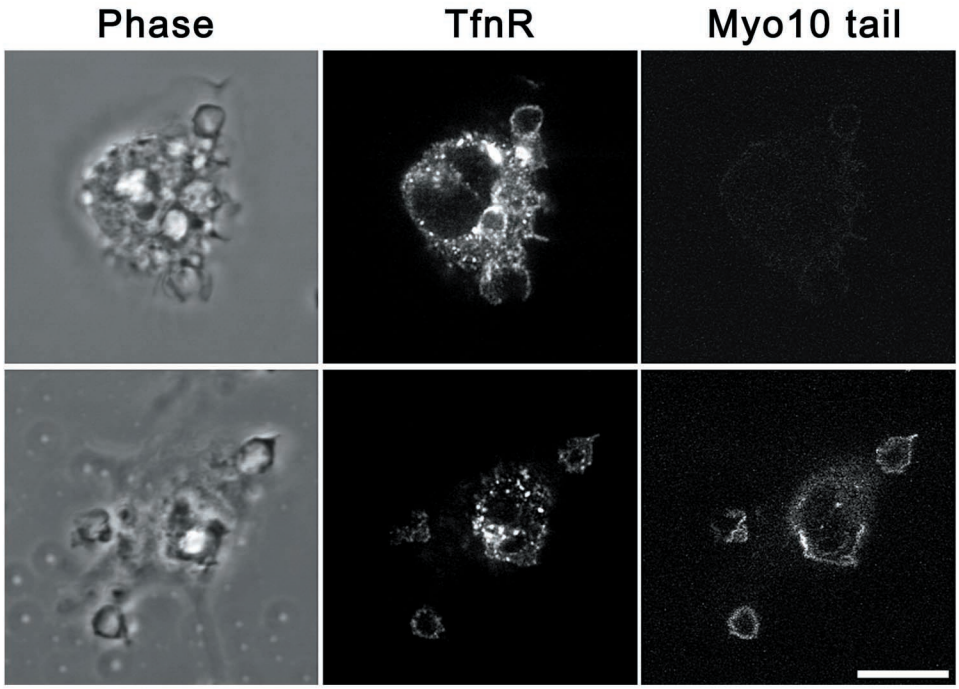

Figure 1 **Expression of Myo10 tail does not inhibit transferrin receptor recruitment to phagocytic cups.** Adherent RAW LR5 cells, transfected with Myo10 tail, were incubated with EIgG for 15 min at 4°C to allow binding but not ingestion, then incubated at 37°C for 2 min. Cells were fixed and stained for transferrin receptors with mAb C2 followed by biotin-conjugated anti rat IgG and rhodamine-streptavidin. Scale bar = 10 μm.

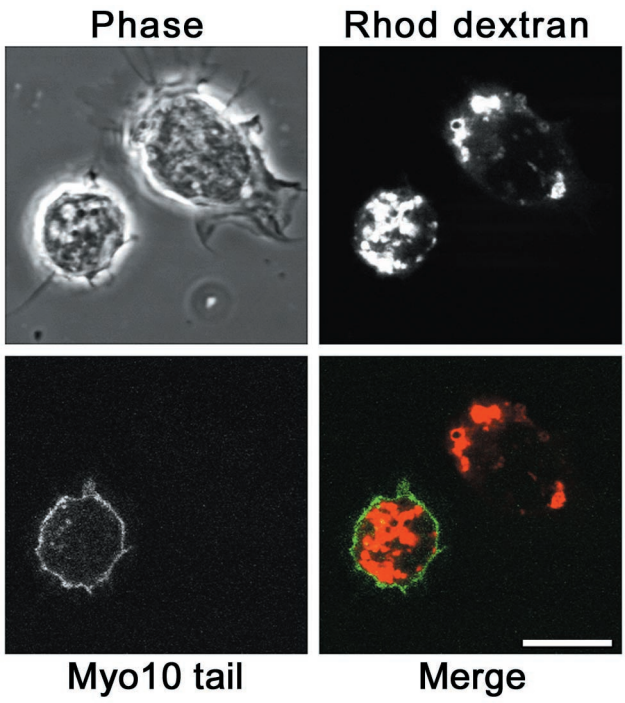

Figure 2 **Expression of Myo10 tail does not inhibit macropinocytosis.** RAW LR5 cells, transfected with Myo10 tail, were incubated in 5 mg/ml rhodamine dextran for 1 hour at 37°C, washed, and allowed to recover in suspension for 1 hour. Cells were then plated on coverslips, fixed and then imaged. Scale bar = 10 μm.